

# THE PHYSICAL REVIEW

*A journal of experimental and theoretical physics established by E. L. Nichols in 1893*

SECOND SERIES, VOL. 112, No. 3

NOVEMBER 1, 1958

## Multipacting Modes of High-Frequency Gaseous Breakdown\*

ALBERT J. HATCH, *Argonne National Laboratory, Lemont, Illinois*

AND

H. BARTEL WILLIAMS, *New Mexico College of Agriculture and Mechanic Arts, State College, New Mexico*

(Received June 23, 1958)

A previously developed average electron theory for the  $\frac{1}{2}$ -cycle multipacting mode of low-pressure, high-frequency breakdown (secondary electron resonance) has been generalized and extended to higher order modes. A semitheoretical plot of breakdown voltage  $V$  vs the product of frequency times electrode separation  $f \times d$  using representative fitting parameters is given for the  $\frac{1}{2}$ - through  $9/2$ -cycle modes. In addition to the customary  $\frac{1}{2}$ -cycle cutoff the theory predicts a modified cutoff in each of the mode transition regions. Breakdown data for internal metal electrodes at 2 microns pressure show the typical  $\frac{1}{2}$ -cycle cutoff at about 100 Mc-cm/sec plus a newly observed  $\frac{3}{2}$ -cycle cutoff as indicated by a dip in the breakdown curve at about 450 Mc-cm/sec. The  $\frac{3}{2}$ -cycle dip exhibits a strong dependence on electrode surface conditions. The theory is compared with multipacting breakdown data from several sources covering a wide range of conditions, including microwave breakdown at sufficiently low pressures.

### I. INTRODUCTION

THE fundamental mode of the multipacting mechanism of low-pressure high-frequency gaseous breakdown, also known as the secondary electron resonance mechanism, is postulated on (a)  $\frac{1}{2}$ -cycle electron transit times between electrodes, and (b) electron multiplication by secondary electron emission at the electrode surfaces. Under appropriate dynamical conditions, multipacting is the dominant high-frequency breakdown mechanism when the electron mean free path exceeds the electrode separation. The possibility of higher order modes was first suggested and briefly investigated by Farnsworth.<sup>1</sup> Gill and von Engel<sup>2</sup> discuss some of the theoretical aspects of the higher order multipacting modes. The most recent studies of the multipacting modes have been made by Krebs and Meerbach,<sup>3</sup> and by Hoover and Smither.<sup>4</sup> Krebs and

Meerbach limited their higher order mode study to theory. Hoover and Smither reported a set of breakdown voltages for a resonant cavity which was consistent with their formulation of the multiple mode theory. The theoretical work of Krebs and Meerbach and of Hoover and Smither has its ultimate portrayal in terms of the time phase angle of secondary electron emission, an internal parameter. Such a portrayal does not lend itself readily to comparison with experimental data.

The purpose of this paper is to generalize and extend the theory of the fundamental and higher order multipacting modes, and to present experimental data which demonstrate newly observed features of these modes. The new portrayal of the theory in terms of the external parameters of applied frequency, electrode separation, and breakdown voltage makes possible the correlation of a wide range of multipacting data, including microwave breakdown.

### II. THEORY

The theory is based on the same postulates and assumptions as our previous formulation of the simple or average electron theory of the  $\frac{1}{2}$ -cycle multipacting mode.<sup>5</sup> The  $\frac{1}{2}$ -cycle transit time, however, is extended to include the higher order modes of  $\frac{3}{2}$ -,  $\frac{5}{2}$ -... cycle transit

\* Supported by the Bureau of Ordnance, U. S. Navy, through cooperation of the Applied Physics Laboratory of the Johns Hopkins University, Silver Spring, Maryland, and by the U. S. Atomic Energy Commission.

<sup>1</sup> P. T. Farnsworth, *J. Franklin Inst.* **218**, 411 (1934).

<sup>2</sup> E. W. B. Gill and A. von Engel, *Proc. Roy. Soc. (London)* **A192**, 446 (1948).

<sup>3</sup> K. Krebs, *Z. angew. Phys.* **2**, 400 (1950); K. Krebs and H. Meerbach, *Ann. Physik* **15**, 189 (1955).

<sup>4</sup> C. W. Hoover, Jr., thesis, Yale University, 1954 (unpublished); C. W. Hoover, Jr., and R. K. Smither, *Phys. Rev.* **98**, 1149 (1955).

<sup>5</sup> A. J. Hatch and H. B. Williams, *J. Appl. Phys.* **25**, 417 (1954).

times. The permitted modes can be represented by transit times of  $(2n-1)\pi$ , where  $n=1, 2, 3, \dots$  is the mode index.

The basic equation of undamped motion for an electron of mass  $m$  and charge  $e$  in a sinusoidal field of peak strength  $E$  and frequency  $f=\omega/2\pi$  is

$$m\ddot{x} = eE \sin\omega t. \quad (1)$$

A first integration of (1) evaluated for the transit-time boundary conditions gives the arrival velocity at the opposite electrode as

$$v_f = \frac{k}{k-1} \left( \frac{2eE}{m} \right) \cos\phi, \quad (2)$$

where  $\phi$  is the time phase angle at which secondary electrons are emitted, and  $k=v_f/v_0$  is the assumed constant ratio of electron arrival velocity to emission velocity as first used by Gill and von Engel.<sup>2</sup> A second integration of (1) evaluated for the resonance boundary conditions gives the multipacting breakdown voltage,

$$V = \frac{4\pi^2 (fd)^2}{(e/m)\Phi_n}, \quad (3)$$

where

$$\Phi_n = \left( \frac{k+1}{k-1} \right) (2n-1)\pi \cos\phi + 2 \sin\phi. \quad (4)$$

The lower breakdown curve limiting phase angle  $\phi_l$  is obtained by maximizing  $\Phi_n$  with respect to  $\phi$ , yielding

$$\phi_l = \tan^{-1} \left[ \frac{k-1}{k+1} \frac{2}{(2n-1)\pi} \right]. \quad (5)$$

A simple fitting procedure involving Eqs. (3), (4), and (5) leads to an evaluation of  $k$ ,  $\phi_l$ , and  $\phi_u$ , the latter representing the upper breakdown curve limiting phase

angle. Finally we can combine the expression for electron arrival energy at an electrode,  $eW_f = \frac{1}{2}mv_f^2$ , with (2) and (3) to obtain

$$fd = \frac{(k-1)\Phi_n}{k \cos\phi} \left( \frac{eW_f}{8m} \right)^{\frac{1}{2}}. \quad (6)$$

This equation is fitted to the cutoff portion of breakdown data to evaluate  $W_{f_l}$ , the electron arrival energy at an electrode for which the effective secondary emission ratio  $\delta=1$ .

Fitting this theory to most of the available data for  $\frac{1}{2}$ -cycle multipacting breakdown by the method outlined previously<sup>5</sup> has yielded the following nominal parameter ranges:  $2.5 \leq k \leq 4$ ;  $+15^\circ \leq \phi_l \leq +20^\circ$ ;  $-60^\circ \leq \phi_u \leq -40^\circ$ ;  $25 \text{ ev} \leq W_{f_l} \leq 100 \text{ ev}$ . On the basis of these figures, one can select representative values of the fitting parameters which can be used to plot a representative set of breakdown curves. These representative values have been chosen as follows:  $k=3$ ;  $\phi_l=17.7^\circ, 6.1^\circ, 3.7^\circ, 2.6^\circ, 2.0^\circ$ , for the  $\frac{1}{2}$ - through  $9/2$ -cycle modes, respectively;  $\phi_u=-58^\circ$ , independent of mode; and  $W_{f_l}=50 \text{ ev}$ . The small changes in  $\phi_l$  for the various modes are a consequence of the theory which appears to have negligible physical significance.<sup>6</sup> In order to complete the simple theoretical description of multipacting breakdown, it is necessary to take into account the existence of an upper limiting  $W_{f_u}$  above which the secondary emission ratio drops below 1. For most metals this value occurs in the nominal range of 2000 to 10 000 ev; a representative value of 5000 ev is chosen. The assumption that  $k$ ,  $\phi_u$ ,  $W_{f_l}$ , and  $W_{f_u}$  are independent of mode order, and can therefore be extrapolated from  $\frac{1}{2}$ -cycle data to the higher order modes, is not completely warranted as will be illustrated by certain aspects of the data which follow. However, it is a plausible first approximation of the multiple-mode problem. If suitable data were available, the fitting parameters could be evaluated independently for each mode. The present data permit quasi-separate modal evaluation of only one fitting parameter,  $W_{f_l}$ .

The multipacting modes in Fig. 1 have been plotted using these representative values of the fitting parameters. Each mode is represented as a completely bounded domain. There is a small separation between the  $\frac{1}{2}$ - and  $\frac{3}{2}$ -cycle domains. For the higher order modes, however, overlapping of the domains is indicated, the extent of the overlap increasing with mode index. The  $\frac{1}{2}$ -cycle cutoff is absolute since for  $fd$  values less than about 80 Mc-cm/sec (dependent on electrode surface conditions), it is impossible to obtain breakdown even with very large rf voltages. The  $\frac{3}{2}$ -cycle cutoff as theoretically

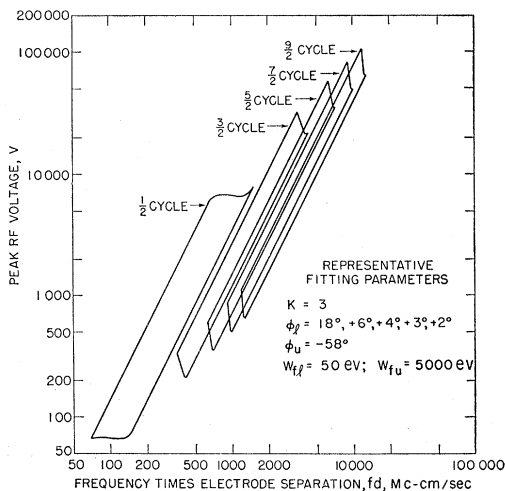


Fig. 1. Multiple mode multipacting theory,  $\frac{1}{2}$ - through  $9/2$ -cycle modes,  $n=1, 2, 3, 4, 5$ .

<sup>6</sup> It can be shown that within the framework of the present theory there is actually a wide range of  $\phi_l$  values instead of the single value used here. This range is several times as great as the small modal changes. A more detailed discussion of this point (which is significant in the electron bunching characteristics of multipacting) is being prepared for publication.

predicted in the vicinity of 400 Mc-cm/sec, however, should be indicated only by a relatively small dip in the lower breakdown curve. The  $\frac{3}{2}$ -cycle cutoff at about 650 Mc-cm/sec, and the succeeding higher mode cutoffs, if they exist, should be indicated by progressively less prominent dips.

### III. EXPERIMENTAL METHOD AND RESULTS

The experimental search for the higher order modes was made with the electrode assembly shown in Fig. 2. This is a demountable system with waxed glass-metal joints. The  $3\frac{1}{2}$ -inch diameter aluminum electrodes were machined with a clean dry tool. No liquid cleaning agents were used. Electrode separation was adjusted by means of the sliding plunger which passed through the O-ring seal. The usable electrode separation range was from about 1 cm to 5.3 cm. Frequencies of 70 and 140 megacycles/sec were used. This combination of electrode separation and frequency provided an  $fd$

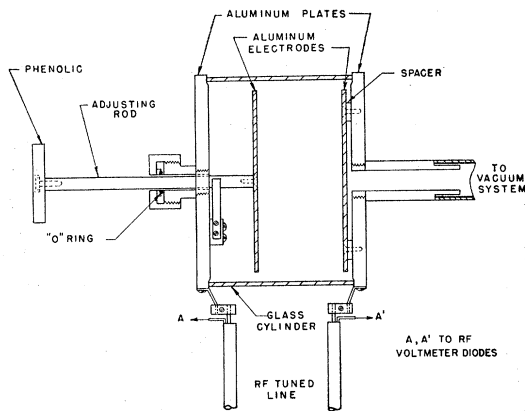


FIG. 2. Breakdown tube with adjustable separation electrodes.

range from 70 to 742 Mc-cm/sec. A double-diode rf voltmeter similar to the one described previously was used.<sup>5</sup> Breakdown voltage measurements were accurate to within  $\pm 5\%$  and precise to within  $\pm 2\%$ . Electrode separation accuracy ranged from 1 to 5%, and frequency accuracy was 1%. The vacuum system included an oil diffusion pump and a dry ice trap. Breakdown was indicated by appearance of glow and sudden lowering of applied voltage.

Observability of the  $\frac{3}{2}$ -cycle cutoff was found to be critically dependent on electrode surface conditions as controlled by outgassing procedure. A sequence of three runs was purposely programed to illustrate this dependence. The breakdown data are shown in Fig. 3. All data were taken at the same pressure, 2 microns Hg, in air. At this pressure, multipacting breakdown voltage is independent of gas pressure. In run No. 1 the electrodes had been partially outgassed by burning the discharge at  $10^{-4}$  mm Hg for half an hour immediately before obtaining data. This procedure brings out a definite dip

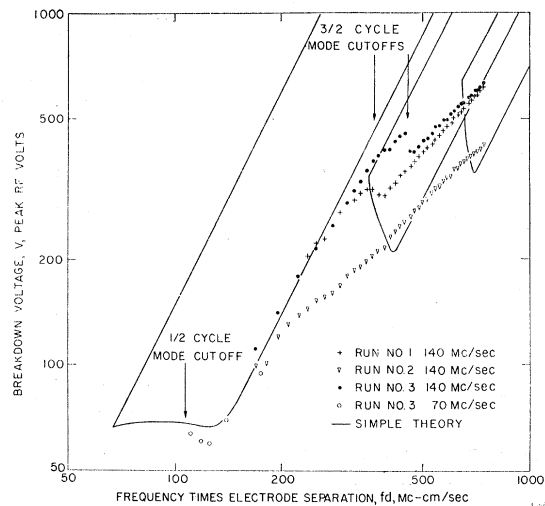


FIG. 3. Multiple mode breakdown data compared with theoretical curves from Fig. 1. Pressure=2 microns Hg for all data.

in breakdown data at about 380 Mc-cm/sec, approximately at the  $\frac{3}{2}$ -cycle theoretical cutoff for  $W_{fi}=50$  ev. In run No. 2 the electrodes had been standing at 2 microns pressure for 24 hours prior to obtaining data and were in an un-outgassed condition. Water vapor was the most likely electrode surface contaminant. There is no evidence of a  $\frac{3}{2}$ -cycle cutoff in this run. In run No. 3 the electrodes were more thoroughly outgassed than in run No. 1 by doubling the outgassing time. The dip in run No. 3 at about 470 Mc-cm/sec is more prominent than in run No. 1 and corresponds to  $\frac{3}{2}$ -cycle theoretical cutoff at about  $W_{fi}=70$  ev. Such a shift of cutoff to higher  $fd$  and  $W_{fi}$  with increased outgassing has been observed previously for the  $\frac{1}{2}$ -cycle mode and is consistent with the well-known reduction in secondary emission yield with progressive stages of outgassing. In run No. 3 the lower portion of the  $\frac{1}{2}$ -cycle breakdown curve was explored down to  $\frac{1}{2}$ -cycle cutoff which occurred at 105 Mc-cm/sec.<sup>7</sup> The lower end of this curve in the vicinity of cutoff fits the theoretical  $\frac{1}{2}$ -cycle cutoff for  $W_{fi}=50$  ev. A confirmatory run through this entire  $fd$  range was then made immediately in the reverse direction. The data for the two directions, including the  $\frac{3}{2}$ -cycle cutoff dip, agreed within the over-all experimental precision of about 3%. Overlap of the 70 and 140 Mc/sec data in run No. 3 is within experimental error limits. The fact that the  $\frac{3}{2}$ -cycle cutoff  $W_{fi}$  is 70 ev compared to 50 ev for  $\frac{1}{2}$ -cycle cutoff in run No. 3 indicates that electron losses in the  $\frac{3}{2}$ -cycle mode are greater than in the  $\frac{1}{2}$ -cycle mode and must be compensated for

<sup>7</sup> The discrepancy between the theoretical and observed cutoff frequencies (80 and 105 Mc-cm/sec in this case) is due in part to oversimplifications in the simple theory and to variable electrode surface conditions. (See reference 5.) Another factor is that in this region multipacting can begin with currents too small to cause a visible glow or lowering of applied rf voltage. A multipacting current threshold curve has been observed to extend to  $fd$  values below the visible glow cutoff, closer to the theoretical cutoff.

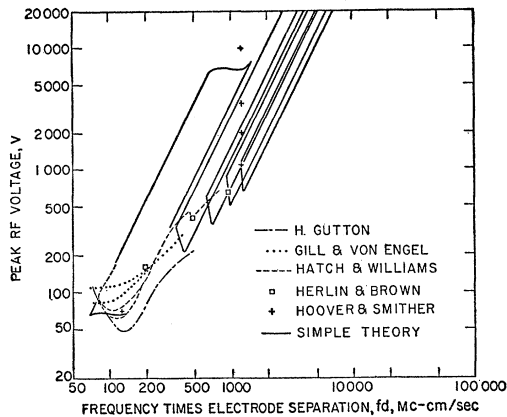


FIG. 4. Comparison of various multipacting data with theory. Electron mean free path exceeds electrode separation for all data.

by a higher secondary emission yield. This dependence of  $W_{fl}$  on mode order also illustrates the remarks in Sec. II regarding the validity of extrapolating  $\frac{1}{2}$ -cycle fitting parameters to the higher order modes. In this case we have assumed that  $k=3$  for all modes and that there is no mode overlapping, neither of these assumptions necessarily representing the actual physical situation.

None of the data in Fig. 3 indicates a  $\frac{5}{2}$ -cycle cutoff. This cutoff may be concealed by mode overlapping, or it may lie outside the  $fd$  range of the experiment. Recent measurements by Davis Philip at New Mexico College of Agriculture and Mechanic Arts, using the apparatus of Fig. 2 with range extended to 1000 Mc-cm/sec, show small dips which are apparently (but not conclusively) due to  $\frac{5}{2}$ - and  $\frac{7}{2}$ -cycle cutoffs. These dips were not consistently reproducible, a feature not at all surprising in view of strong dependence of the  $\frac{1}{2}$ - and  $\frac{3}{2}$ -cycle mode cutoffs on electrode surface conditions.

#### IV. DISCUSSION OF RESULTS

The experimental breakdown data exhibit two distinct slopes. In run No. 2 the slope is approximately 1 for all of the data. In runs No. 1 and No. 3 the slope changes just below the  $\frac{3}{2}$ -cycle cutoff. In the major portion of the  $\frac{1}{2}$ -cycle mode data for runs 1 and 3, the slope is approximately 2 on the log-log plot, in accordance with the  $\frac{1}{2}$ -cycle theory,  $V \propto (fd)^2$ . As the  $\frac{3}{2}$ -cycle cutoff is approached from the  $\frac{1}{2}$ -cycle side, however, the slope changes to approximately 1,  $V \propto (fd)^1$ . The slope of both the first and third runs above the  $\frac{3}{2}$ -cycle cutoff is also 1. This unity slope is approximately the same as that of the envelope of the higher mode curves. Thus, the existence of unity slope appears to be associated with mode overlapping. A possible theoretical representation of mode overlapping can be obtained by eliminating the mode parameter  $\Phi_n$  from Eqs. (3) and (6). This gives

the breakdown voltage as

$$V = \left[ \frac{(k-1)\pi}{k \cos\phi} \left( \frac{2W_f}{e/m} \right)^{\frac{1}{2}} \right] fd. \quad (7)$$

This relation can also be obtained by eliminating  $v_f$  from Eq. (2) and the energy relation  $eW_f = \frac{1}{2}mv_f^2$ . Equation (7) can be fitted to the slope 1 portion of the breakdown curves by letting the bracket be a constant,  $V = \text{const} \times fd$ . In this case we obtain  $V = 0.85fd$ . Any determination of the internal parameters  $k$ ,  $\phi$ , and  $W_f$  within the brackets appears to be without significance.

#### V. CORRELATION WITH OTHER DATA

The generality of the multipacting variables  $V$  and  $fd$  makes possible the ready comparison of multipacting data covering a wide range of conditions.

In Fig. 4 are plotted experimental multipacting breakdown curves and data points selected from several sources along with a portion of the theoretical curves from Fig. 1. All data in this figure were taken at pressures sufficiently low to satisfy the electron mean free path requirement for multipacting. The Gutton curve for glass electrodes at 5-cm separation is from the original observations on multipacting.<sup>8</sup> We are unable to find any reason for the factor of 2 difference between the data of the Guttons and other multipacting data. The change in slope at about 300 Mc-cm/sec appears to indicate a transition from  $\frac{1}{2}$ -cycle mode operation to an overlapping  $\frac{1}{2}$ - and  $\frac{3}{2}$ -cycle mode operation. The Gill and von Engel curves are also for glass electrodes at separations of 3 and 6 cm. Their curves are higher than the representative theoretical curve in the cutoff region, a result which can be explained on the basis of the lower secondary emission yield for glass compared with metals. The two curves of the present authors are for metal electrodes. Included are run No. 3 of Fig. 3, and a partially closed breakdown curve for 3-cm electrode separation as previously reported (Fig. 4 of reference 5, partially overlapping run No. 3).

The Hoover and Smither's<sup>4</sup> data are of interest in that they represent multipacting in a heavy-particle rf linear accelerator rather than in a system designed especially for basic breakdown studies. Multipacting breakdown in this case was observed in a 50-Mc/sec re-entrant cylindrical copper-lined cavity. Breakdown occurred at 70 volts in a 2.54-cm gap, and at 1100, 2000, 3500, and 10 000 volts in a 25.4-cm gap. The 70-volt value fits the  $\frac{1}{2}$ -cycle mode curve at 125 Mc-cm/sec; the succeeding voltages can be associated with the  $\frac{3}{2}$ -,  $\frac{5}{2}$ -,  $\frac{7}{2}$ - and  $\frac{9}{2}$ -cycle modes, respectively, at 1250 Mc-cm/sec. The distinctness with which these modes were observed can be attributed to several factors. Among these were the inherent high sensitivity of their high- $Q$  cavity to the load imposed by multipacting, the use of dc bias to eliminate unwanted modes, and the availability of rf

<sup>8</sup> H. Gutton, Ann. phys. 13, 62 (1930).

power in the kilowatt range. All the above data are for frequencies in the 10- to 140-Mc/sec range and for electrode separations from 1 to 10 cm.

Finally, the Herlin and Brown<sup>9</sup> data show that multipacting can be the dominant microwave breakdown mechanism at pressures below the mean free path limit of the diffusion mechanism.<sup>10</sup> Their breakdown data for 3125 Mc/sec (Fig. 2 in reference 9) indicate that at a pressure of about 0.1 mm Hg in air the field strength vs pressure curves tend to level off to steady values. From Herlin and Brown's curves we have determined these values as listed in column 3 of Table I. The electrode separations and corresponding  $fd$  values are listed in columns 1 and 2, respectively. The breakdown  $V$  values in peak volts in column 4 are obtained from column 1 and the rms  $E$  values of column 3. The kinetic-

<sup>9</sup> M. A. Herlin and S. C. Brown, Phys. Rev. **74**, 291 (1948).

<sup>10</sup> S. C. Brown and A. D. MacDonald, Phys. Rev. **76**, 1629 (1949).

TABLE I. Low-pressure extrapolation of microwave breakdown data showing multipacting characteristics (adapted from Herlin and Brown<sup>a</sup>).

Electrode separation $d$ , cm	$fd$ , Mc-cm/sec	Breakdown $E$ , rms volts/cm	Breakdown $V$ , peak volts
0.0635	200	1800	160
0.157	490	1800	400
0.318	990	1500	670

<sup>a</sup> See reference 9.

theory mean free path for electrons in air at this pressure is about 0.5 cm, longer than any of the electrode separations used. The  $V$  and  $fd$  values from this table are plotted in Fig. 4. The three points appear to correspond to  $\frac{1}{2}$ -,  $\frac{3}{2}$ -, and  $\frac{5}{2}$ -cycle multipacting. The emergence of multipacting as the dominant mechanism at sufficiently low pressures is similarly evident in other microwave breakdown data.

### Energy-Band Interpolation Scheme Based on a Pseudopotential

JAMES C. PHILLIPS

*Bell Telephone Laboratories, Murray Hill, New Jersey*

(Received July 14, 1958)

In this paper an interpolation scheme is developed that depends on only a few parameters. This is done by observing that the effective potential for electrons near the Fermi level can be split into two parts, the part due to the core, and the part due to the other valence electrons. It is assumed that for semiconductors the relative effect of the core is small, so that it can be replaced by an effective repulsive potential. In this way two-parameter pseudopotentials are constructed for diamond and Si that give good agreement with orthogonalized plane wave calculations and experiment at special points of the Brillouin zone, and also yield reasonable results for the bands at other points of the zone. A by-product of the calculations is the discovery of an error in the model for the valence bands of Si near the center of the zone proposed by Dresselhaus. A compromise model is proposed in good agreement with theory and experiment. Good results are obtained for Ge with a three-parameter pseudopotential. Finally, the many experimental facts that have been deduced about the band structures of Si and Ge are augmented by the results of the pseudopotential calculations to yield fairly accurate ( $\delta E \lesssim 0.05$  ry) sketches of the energy bands of these crystals along the [100] and [111] directions in the neighborhood of the energy gap.

#### 1. INTRODUCTION

THE complete determination of the electronic energy bands of a solid requires knowledge of the energy  $E$  in the  $i$ th branch, for all  $i$  of interest, and for all wave vectors  $\mathbf{k}$  of the Brillouin zone. In practice most calculations have determined  $E_i(\mathbf{k})$  only for wave vectors  $\mathbf{k}$  possessing a sufficiently high symmetry. In such cases group theory<sup>1,2</sup> can be used to reduce the order of the secular equation. It has been found<sup>2</sup> that in semiconductors even the points of highest symmetry, such as  $\mathbf{k}=0$ , require the solution of approximately  $10 \times 10$  secular equations. Thus a convergent solution at other points of the Brillouin zone is not easily

obtained. In addition, the  $E(\mathbf{k})$  curves are known<sup>1</sup> to be smooth functions of  $\mathbf{k}$ , so that if one knew  $E_i(\mathbf{k})$  at two symmetry points, one would be tempted to interpolate between them, at least along the symmetry line connecting them.

For these reasons Slater and Koster<sup>3</sup> proposed an interpolation scheme based on the tight-binding approximation. They pointed out that if the various overlap integrals occurring in the tight-binding formalism are regarded as disposable parameters, the matrix elements of the secular equation will have, as a function of  $\mathbf{k}$ , a simple analytic form. The parameters are then determined by fitting energy values determined by cellular or orthogonalized plane wave treatments at symmetry points. While this viewpoint is appropriate

<sup>1</sup> Bouckaert, Smoluchowski, and Wigner, Phys. Rev. **50**, 58 (1936).

<sup>2</sup> F. Herman, Phys. Rev. **88**, 1210 (1952); **93**, 1214 (1954).

<sup>3</sup> J. C. Slater and G. F. Koster, Phys. Rev. **94**, 1498 (1954).